2
Materials and Metallurgy

Tim J. Band

My first involvement with metal on metal bearings was in 1995. Corin Medical Ltd (Circencester, UK). asked Centaur Precision Castings Ltd (Sheffield, UK) to take over the supply of castings for the McMinn resurfacing from Trucast (Isle of Wight, UK). As the Medical Development Manager at Centaur, my engineering team and I took on that project.

Without specifications available for the device, with the exception of the material specification, ISO 5832 part 4 (formerly BS3531 and BS7252) and ASTM F75 (Tables 2.1 and 2.2), reverse engineering principles were used to identify the casting methods employed for the earlier product produced at Trucast. This included sectioning of castings to determine their grain structure and microstructure, which would allow the identification of the casting process used for the earlier product.

This forensic analysis of McMinn metal on metal hip resurfacing castings resulted in identifying that there had been a number of process methods employed in the manufacturing of these products, which had resulted in variable microstructures in the castings.

The range included the as-cast microstructure, without thermal treatment, single heat treatment of a solution heat treatment (SHT) or hot isostatic pressing (HIP), and both SHT and HIP (Fig. 2.1). The details of these treatments and their effect on the microstructure of cobalt chromium molybdenum alloy will be described later in this chapter. However, it is opportune to draw the reader's attention to the marked effect that the thermal treatment has on the microstructure, which is evidenced by the different morphology present. When these microstructural conditions had been identified, and their casting processes determined, Centaur Precision initiated the validation and approval submission documents for the McMinn metal on metal hip resurfacing castings that reproduced the structures identified in the Trucast product.

The difficulty in manufacturing the McMinn resurfacing was that the acetabular cup component had a superomedial peg that was approximately 15 mm long, 10 mm in diameter, and had splines that ran longitudinally down its length (Fig. 2.2). The convex surface of the cup also had a stippled textured surface and antirotation fins that restricted the opportunity for *gating* positions, which are an essential aspect of the investment casting process; this will also be explained later in the chapter. In order to produce as many of the surface details without the need for machining, the gating position had been located on the top of the superomedial peg as can be seen by the fan-shaped feature in the image.

This gating position created a narrow passage for the liquid metal to flow into the acetabular cup cavity and resulted in insufficient metal being available in the cup cavity after the peg metal solidified, preventing effective liquid metal *feeding* from the runner system. This resulted in microporosity, or voids, in the metal when the liquid-to-solid metal transfer occurred at the solidification temperature (Fig. 2.3).These microporosity pores, though not significantly detrimental to the mechanical properties of the casting, represented a cause of reduced manufacturing yields as negative pores can get exposed on the polished bearing surface after machining and polishing. It appears that this had been the main reason that Trucast had introduced the HIP process, which, through the application of temperature and pressure, can remove the porosity from the metal microstructure. A detailed description of the casting process and the resultant microstructures was submitted to the medical design and development team at Corin for review and subsequent approval. The dual thermal process was adopted at Centaur Precision after validation of the casting process. Mr. McMinn was not involved in any of these decisions. Centaur was a supplier to Corin, and we assumed that Corin would have made the designer aware of process changes to his implant.

It was during 1996 and early 1997 when Derek McMinn had cause to independently investigate the product produced by Corin Medical that he identified that the material of his resurfacing device had been altered without his knowledge or consent. His original request was that the material should replicate that of the successful first-generation metal on metal bearings. It was these that had provided him with the idea of reintroducing hip resurfacing with this appropriate material, which had enjoyed more than 30 years of benign clinical

TABLE 2.1. Chemical composition

Element	Compositional limits, % (*m/m*)
Chromium	26,5 to 30,0
Molybdenum	4,5 to 7,0
Nickel	1,0 max.
Iron	1,0 max.
Carbon	0,35 max.
Manganese	1,0 max.
Silicon	1,0 max.
Cobalt	Balance

use. Without understanding the relevance of this change at the time, Mr. McMinn conducted a review of available literature on the subject of thermal treatments of cobalt chromium molybdenum alloy. He found that whereas these heat treatments produced an improvement in mechanical properties such as fatigue strength, and rendered the material easier to machine, a big downside was that they led to a reduction in its wear properties. Of course, it was the wear properties of the alloy that had been the attraction of this material. For a variety of reasons, the McMinn resurfacing hip prosthesis was withdrawn from use, and the fate of these prostheses is described elsewhere in this book.

If one considered introducing another metal on metal bearing at this time, you could have been excused for thinking that the limitation of the specification, with regard to material, was one of bulk chemical composition only, as there were a number of material wear test reports from reputable test houses suggesting that most variations and combinations of CoCrMo alloy would provide comparable durability. It was even suggested that the carbon content of the alloy, that is to say, high-carbon (C>0.2%) or low-carbon (C<0.07%) alloys,

TABLE 2.2. Chemical composition

	Composition, % (Mass/Mass)	
Element	min	max
Chromium	27.00	30.00
Molybdenum	5.00	7.00
Nickel	…	0.50
Iron	…	0.75
Carbon	…	0.35
Silicon	…	1.00
Manganese	…	1.00
Tungsten	…	0.20
Phosphorous	…	0.020
Sulfur	…	0.010
Nitrogen	…	0.25
Aluminum	…	0.10
Titanium	…	0.10
Boron	…	0.010
Cobalt[A]	balance	balance

[A] Approximately equal to the difference of 100% and the sum percentage of the other specified elements. The percentage of the cobalt difference is not required to be reported.

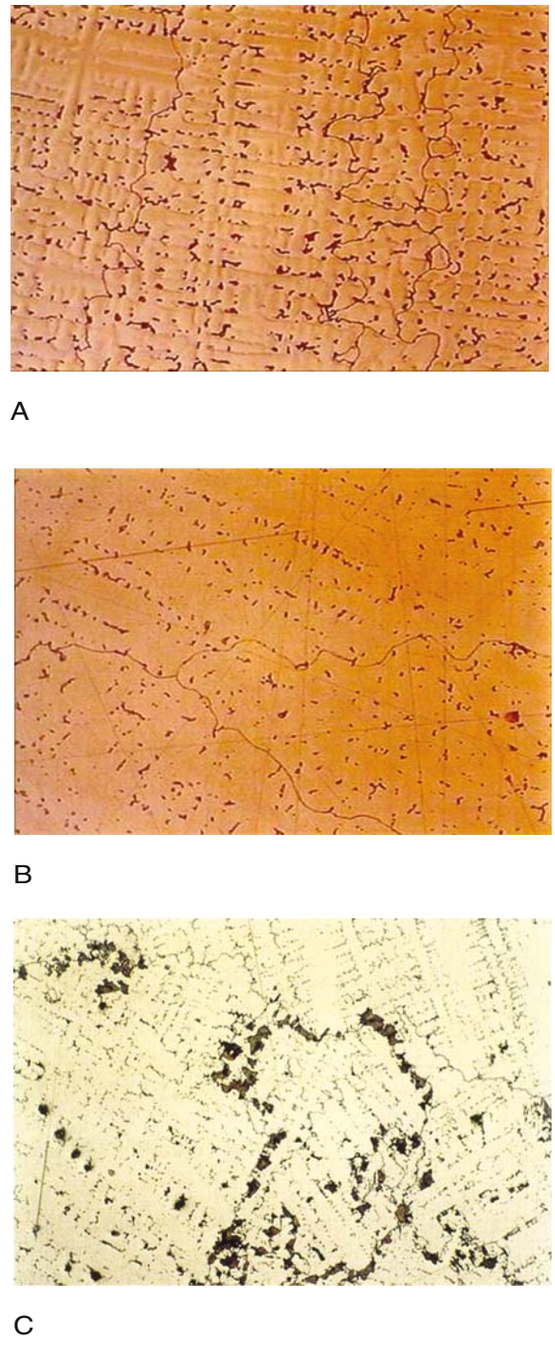

FIG. 2.1. (A) As-cast. (B) Single solution heat treatment (SHT). (C) Hot isostatic pressing (HIP).

behaved with the same performance in hip simulators [1]. This helped to support the introduction of future bearings, as CoCrMo alloy is more easily machined if the carbon content is low or if the carbon is not allowed to precipitate in a coarse form during casting solidification.

When the design of the Birmingham Hip Resurfacing (BHR) device commenced, it included the formalizing of a

FIG. 2.2. McMinn resurfacing acetabular cup casting.

detailed specification that included material, microstructural, and geometric characterization of both the femoral head and acetabular cup components. On this occasion, when Midland Medical Technologies (MMT) provided specimens of the first-generation metal on metal devices that had worked well for many decades, they insisted upon a detailed forensic analysis.

The forensic study of these first-generation metal on metal bearings, the Ring and McKee-Farrar devices (Fig. 2.4), included bulk chemical analysis, surface examination and characterization to determine the surface topography and the wear mechanism of the material, inspection and measurement of profiles to determine the sphericity, clearance (difference between the head and cup size), wear of the articulating surfaces, and sectioning of the articulating surfaces to examine and determine the metallurgical structure of the components.

It was important to consider, while conducting the forensic analysis, that the first-generation metal on metal devices had been produced as two-piece components that were welded together to allow the head to be a hollow component, reducing the component weight and eliminating the difficulties in

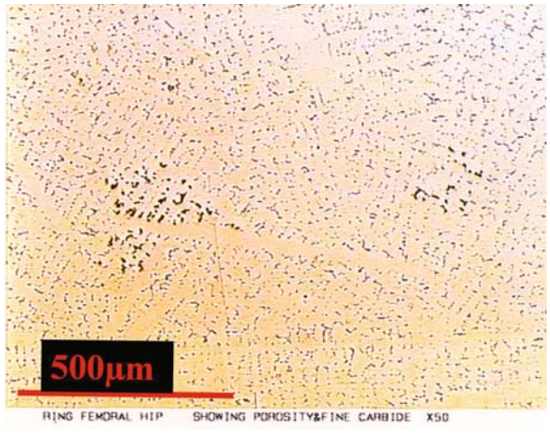

FIG 2.3. Micrograph showing microporosity in the microstructure.

A

B

FIG. 2.4. (A) Ring metal on metal hip prosthesis. (B) McKeeFarrar metal on metal hip prosthesis.

producing large thick sections during the casting process. The weld line that joined the head cap to the stem was a narrow band close to the equator of the femoral bearing and away from the intended articulation area (Fig. 2.5). The original welding would have used a filler wire produced from cobalt chrome alloy, whereas contemporary welding of two-piece femoral devices uses electron beam welding (EBW), which melts and fuses positive ribs produced on the host component to avoid *sinking* of the casting profile during welding.

The forensic analysis of these devices took place between Centaur Precision and the Materials Research Institute (MRI) at the Sheffield Hallam University, where there was a combined resource of experts in the fields of engineering of orthopedic devices, investment casting, and metallurgy. Particularly helpful in this exercise were Graham Dixon, chief metallurgist at Centaur, and John Metcalf and Dr. Jess Cawley, who were scientists at MRI. Bulk chemical analysis identified the material as cobalt chromium molybdenum alloy, where the

FIG. 2.5. Cross section of a two-piece assembly of the hollow femoral device in an electron beam welded condition.

chromium content was ~28% to 30%, molybdenum content was ~5% to 7%, carbon was 0.20% to 0.35% by weight, and the balance was cobalt. Other elements in smaller amounts were identified as nickel, silicon, manganese, nitrogen, and iron with other trace elements such as aluminum, titanium, sulfur, and phosphorus. The microstructural characteristics of the material, identified through metallography, revealed a biphasic structure (Fig. 2.6). This was where the matrix of the material, rich in cobalt with chromium and molybdenum, supported a second metallurgical phase carbide that was rich in chromium, molybdenum, and carbon.

The carbide phase had a coarse block morphology and was similar to Chinese script in its shape (Fig. 2.7). This was due to the fact that the carbide particulate is the last liquid to solidify

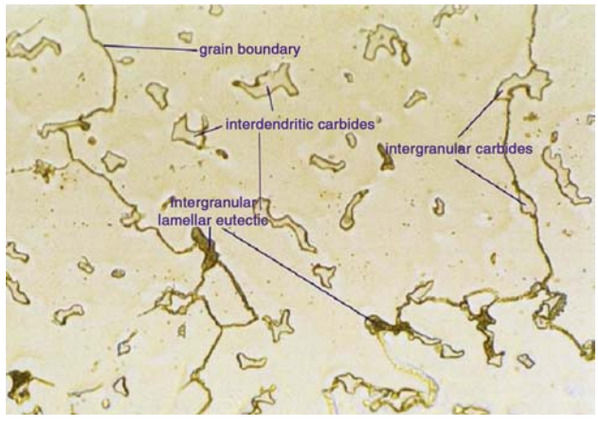

FIG. 2.6. As-cast microstructure showing biphasic structure of carbide and matrix.

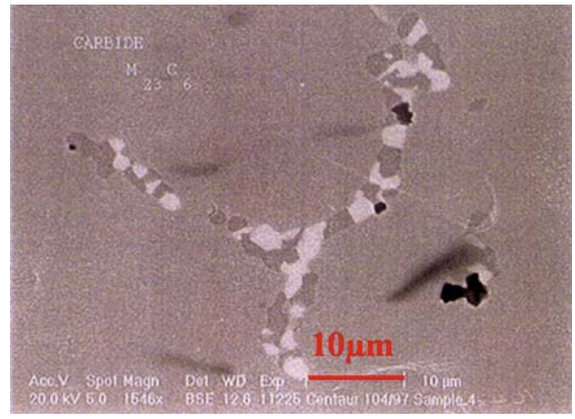

FIG. 2.7. Micrograph showing as-cast, block carbide in the interdendritic pattern.

in the casting process as it is the lowest melting point solute in the interdendrite spaces. The solidification process of this alloy system will be described in more detail later in this chapter.

Surface characterization using low-power optical microscopy identified surfaces that were predominately measured as a negative skew, where there were more scratches than asperities on the surface, in an area that had experienced wear. The scratches on the worn areas of approximately 2 to 3 µm in width were indications of an abrasive wear process as the scratches were seen to be in the intercarbide spacings of the matrix material. These were most probably due to fractured carbide particles acting as third-body wear components as the wear process evolved (Fig. 2.8). There was evidence that the carbide component resisted abrasive wear, in that it can be seen on micrographs that scratches terminate when they meet a carbide in the matrix (Fig. 2.9).

At the same time, in areas where no wear had been experienced, such as the inferior medial zone of the femoral head, the surfaces were found to be in their original manufactured condition of more than 30 years earlier and were found to have a positive skew, with more asperities than scratches on the surface. This phenomenon is described as *relief polishing* in manufacturing terms and is the term used to describe a softer matrix material being worn at a faster rate than is a

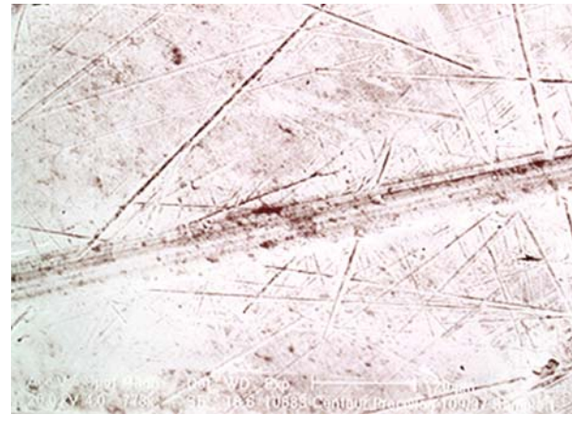

FIG. 2.8. Scratches on bearing surface.

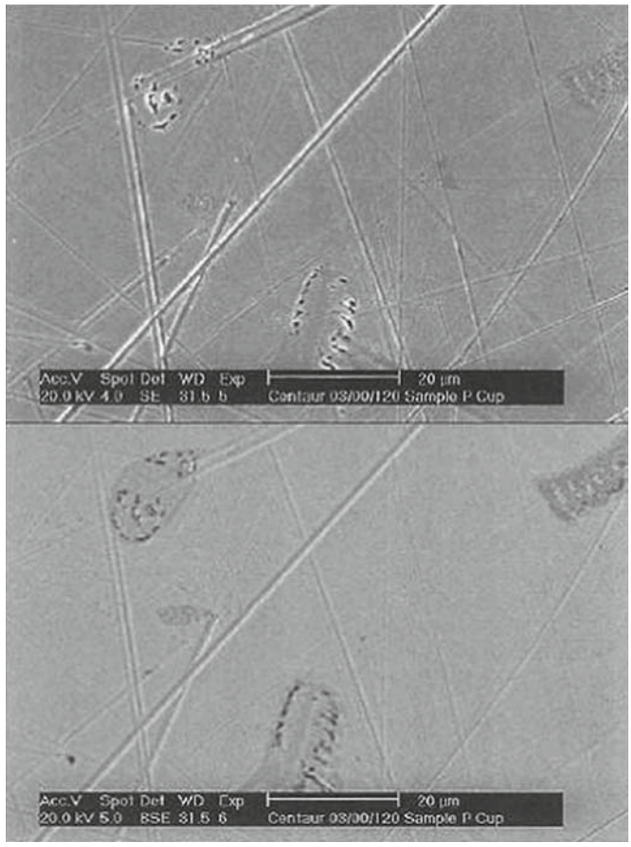

FIG. 2.9. Termination of scratches at carbide junctions.

harder second metallurgical phase that stands proud of the matrix surface due to its resistance to wear. This is similar to the hard rings and knots found in hardwoods when polishing takes place resulting in high points on the polished surface.

To conduct further analysis of the surfaces, an analytical technique called noncontact surface profilometry was used to measure the surface contours at a nanometric level and to provide a representation of the surface in three-dimensional images (Fig. 2.10).

These measurements confirmed that the unworn, as manufactured, surfaces had peaks of up to 100 nm (0.1 µm, or 0.0001 mm) that were coincidental with the carbide distribution seen in the optical micrographs. On the worn surfaces, the scratches were easily identified. It could be seen that the scratch edges had small ridges indicating that the material had undergone plastic deformation rather than having had a strip of material removed, which occurs in the machining process. The CoCrMo alloy system had already been described as having a *self-polishing* capability, which was further confirmed when evidence of multiple scratch paths crossing each other showed a softening of the ridges at the edge of the earliest scratch on the micrograph by the passage of a later scratch. This can also be seen on Figs. 2.8 and 2.9.

More extensive metallurgical examination took place by examining the bearing surfaces using scanning electron microscopy (SEM). Many weeks, days, and hours were spent at MRI in Sheffield examining these precious retrieved specimens that held the key to the durable bearing solution. When

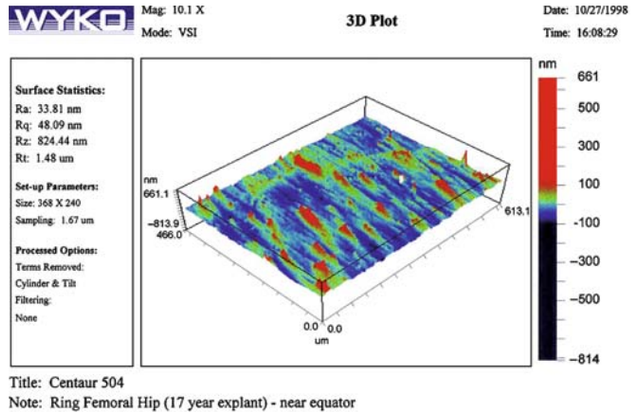

FIG. 2.10. Noncontact profilometry of the as-cast surface showing asperities coincidental with the carbide of 100 nm.

examining the material using secondary electron imaging, there is an opportunity to see surface discontinuities and some topographical features. However, this technique does not measure height, depth, or give any indication of whether or not one is looking at a positive or negative feature on the surface. It was always important to consider this in context with the earlier examination to avoid confusion or misinterpretation. By looking at the same field of view but using backscatter electron imaging (BSE), it was possible to see the contrast in atomic mass of the elements in the microstructure and therefore determine the presence, morphology, and distribution of the metallurgical phases in the microstructure. Through elemental mapping, it was determined that the carbide phase in this biphasic material was rich in chromium, molybdenum, and carbon and that the matrix was predominately cobalt, chromium, and molybdenum, the latter two elements being in lower concentrations than in the carbide phase. The contrast in atomic mass between the chromium-rich and the molybdenum-rich carbide phase can be seen in Fig. 2.11,which was

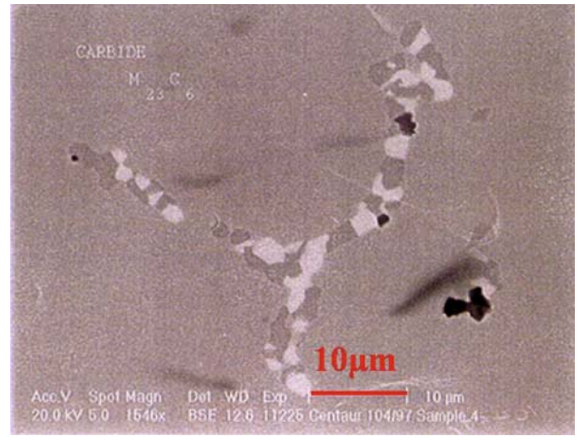

FIG. 2.11. Micrograph showing as-cast, block carbide with molybdenum-rich (light phase) and chromium-rich (dark phase) areas in the carbide.

previously used to show the Chinese script form of the carbide, where the molybdenum is lighter in contrast, because of its heavier atomic mass, when compared with chromium or the surrounding matrix. The carbide phase within the matrix was determined, by phase proportion analysis to occupy between 4% and 5% of the field of view and was of a large block morphology. The size of the carbides were observed to be 2 to 3 µm wide and 10 to 30 µm long, following the pattern of the dendritic structure of the matrix. It was comforting to see the consistency and similarity of the microstructures of these first-generation metal on metal bearings as this was leading toward the development of a sensible material specification.

Further detailed metallurgical analysis of the bearing material was carried out by sectioning the material and preparing specimens for microstructural examination. Care was taken when examining the femoral devices to ensure that observations were made on representative sections of the two-piece assembly previously described. It was by using transmission electron microscopy (TEM) that the real structure of the material could be determined, which was extremely important in determining how these components had been manufactured more than 30 years earlier. The bright-field images recorded during TEM examination revealed that the matrix was a face-centered-cubic, austenitic structure and that the carbide was an $M_{23}C_6$ type carbide, where M represents the metal elements of Cr and Mo, and C represents carbon (Fig. 2.12).

The atoms of chromium, cobalt, and molybdenum are of a similar size, with goldschmidt atomic radii of ~130 to 140 angstroms (Å), and at temperatures below ~1230°C form a solid-state solution where they arrange themselves in an organized face-centered-cubic structure, or lattice, but with random element positioning within the structure (Fig. 2.13). The carbon atom is approximately half the size of these other atoms and is described as an interstitial atom that occupies discontinuities, vacancies, or faults in the lattice. This was

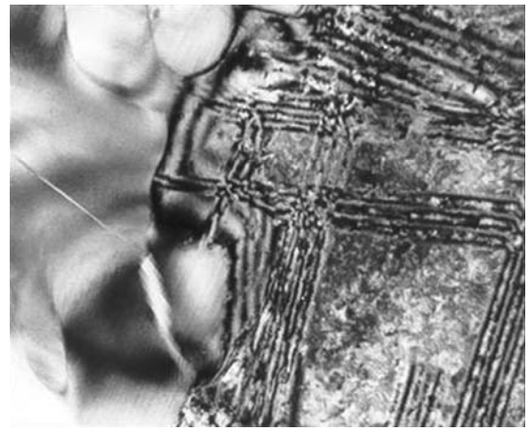

A

B

FIG. 2.12. (A) Bright-field TEM image of the matrix in as-cast CoCr. (B) Bright-field TEM image of the carbide phase in as-cast CoCr.

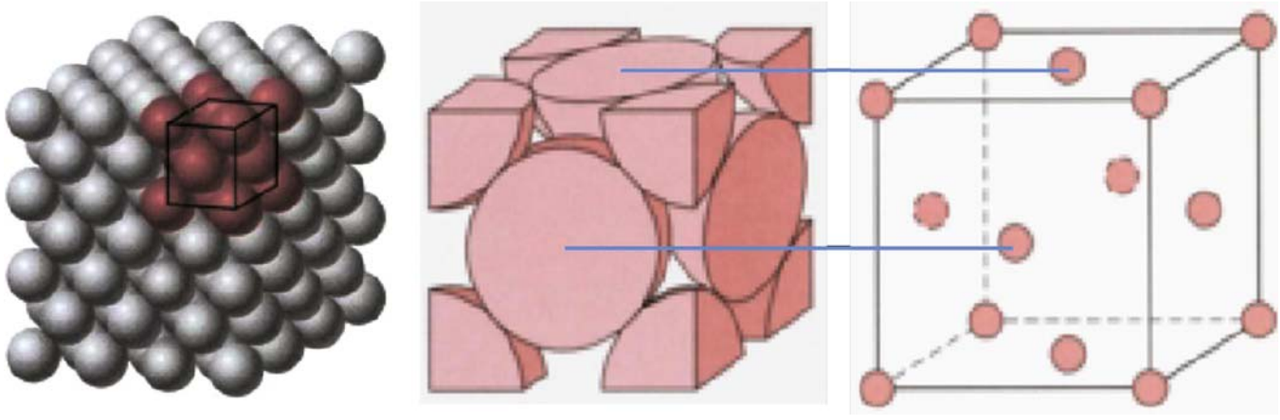

FIG. 2.13. Atoms in a face-centered-cubic (FCC) lattice structure.

further confirmed when the electron diffraction patterns and kikuchi lines, recorded during electron backscatter detection (EBSD), where electrons are passed through a thin film of the material, were solved through identifying the planes and orientations of the atoms in the structure (Fig. 2.14).

Although CoCr is predominately a face-centered-cubic, austenitic alloy system, it has been hypothesized that during work-hardening (which can occur during final stages of the machining and finishing processes as well as during articulation) of the bearing surface, a metallurgical phase change occurs where the face-centered-cubic structure is modified into a hexagonal close-packed (HCP) structure. Because of the extremely narrow affected zone, it is necessary to use TEM to determine this change. Although this transformation in cobalt alloys is not well understood and cannot be precisely controlled, it remains a variable contributor to the wear process of CoCr bearing materials.

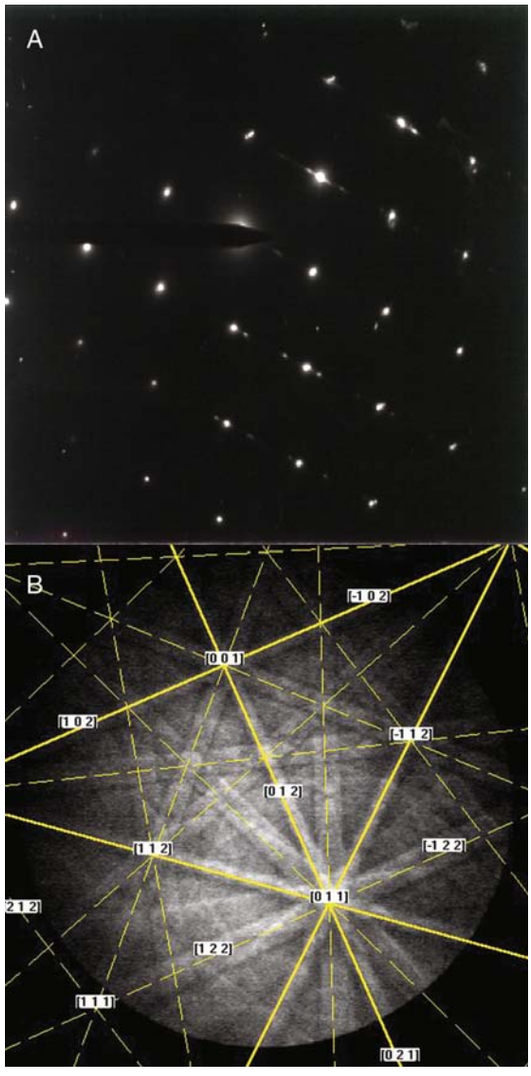

FIG. 2.14. (A) Electron diffraction pattern of face-centered-cubic CoCr and (B) solved kikuchi lines to diffraction pattern of carbide.

It was quite remarkable how similar the metallurgical characteristics of these first-generation metal on metal bearings were. The forensic analysis had identified that the devices had been produced in high-carbon cobalt chromium alloy and from the investment casting process. The casting process of the high-carbon-containing alloy had allowed sufficient time for the precipitation of the large block carbides, which suggested that no *forced cooling* of the casting took place after the metal pouring process. A forced cooling process is a post-cast technique often employed to develop a finer grain structure in casting alloys, for improved mechanical and fatigue strength, and shortens the solidification range (time to cross between liquidus and solidus temperature and phases), which reduces the time for carbides to precipitate. The evidence of low wear, of the order 2 μm of linear wear per year *in vivo*, lower wear on the cup than on the head, and a comparable microstructure on both articulating surfaces suggested that the femoral head device had been marginally subservient to the acetabular cup device. This is most likely due to the nature of a polar bearing contact, with the contact surface area of the head articulating on a larger equivalent contact surface area of the cup, demonstrating that the parity in microstructure had not been a subservient variable in the articulating pair.

Having identified these material, microstructural, and geometric characteristics from the retrievals, it was possible to develop a specification for the controlling features of the BHR device. The formalizing of a specification at this stage would ensure that product conformance and repeatability would be ensured through the application of quality accredited manufacturing and inspection processes, which had not been in place when the original metal on metal bearings were produced. It had been, in part, due to the variability in the manufacturing processes employed more than 30 years before these devices were examined that a number of early failures had been experienced. The product dimensional and geometric variability had resulted in suboptimal bearing conditions, developing high frictional torques, loosening, and wear. The development of a specification based on the forensic analysis, determining the critical factors leading to the good long-term clinical results of the first-generation bearings, was intuitively the right approach as there would be no "new" variables in the design that could not be linked to a prior accepted experience in clinical use. Any variation to these characteristics would have to be considered untried and untested, and therefore their introduction would have to be considered a risk factor to the longevity and benign clinical acceptance of the bearing.

The characteristics of the forensic studies of the successful first-generation metal on metal bearings were that they were produced from high-carbon-containing cobalt chromium molybdenum alloy and were produced in the as-cast microstructural condition. Both bearing components of the articulation were found to be produced in the same metallurgical condition with a cobalt, chromium, molybdenum matrix

supporting interdendritic block carbides of $M_{23}C_6$. The atoms are both ionically and covalently bonded in the carbide precipitate phase.

Casting Method

The first-generation metal on metal bearing components, such as the Ring, McKee-Farrar, Huggler, and Muller devices, were produced from the investment casting process. The investment casting process is one of the oldest metal-forming processes in history with origins dating back more than 4000 years. For those readers with further interest, I recommend a concise text by Beeley and Smart, entitled *Investment Casting* (ISBN 0 901716 66 9). The term *investment casting* is derived from the characteristic use of mobile ceramic slurries, or *investments*, to form molds with extremely smooth surfaces. Another description of the process is *the lost wax process*, where the facsimile, or copy, of the final design is produced from a wax pattern that is sacrificed later in the process after it has been used to produce a cavity inside the ceramic mold.

A major advantage of the casting process is that detailed features can be produced, which reduces significant machining time and costs of the final device. The process begins by producing a facsimile of the final component in wax. This wax pattern can be produced by machining a cavity into a wax pattern tool, or die, which allows molten wax to be injected into the cavity to form the pattern shape (Fig. 2.15).

Investment casting engineers have to consider the complexity of the shapes, and details to be cast in, to design the wax pattern tool to allow the wax pattern to be produced and removed from the tool cavity without distortion of the form. Detailed surfaces, passages, and or channels in the casting can be produced using either soluble wax cores or ceramic cores, but the relative simplicity of the detail on the first-generation metal on metal bearings did not require any complex tooling or core design to be used. If ceramic or soluble cores are used, then they are produced as prefabricated objects with a core print having similar constraints as a casting gate. The core print is used to locate the core inside the wax pattern tool so that when the wax is injected into the tool cavity, the wax surrounds the core except for the print, which is located outside the tool cavity, and the core becomes a secure feature inside the wax pattern. In the case of soluble wax cores, these are dissolved out of the wax pattern. The resultant recessed feature, or cavity, is invested in the standard shelling process, whereas in the case of a ceramic core, the core print/wax pattern junction is sealed prior to investment. Then, after dewaxing, the ceramic core is located in the ceramic shell awaiting the pouring of molten metal around the core feature. This ceramic material is later removed from the casting by a chemical leaching process, leaving the casting with detailed features that otherwise would not be producible or would be very costly to machine. Ceramic cores are used to produce the introducer threaded holes on the BHR acetabular cup. The core print locations can be seen in the wax pattern tool shown in Fig. 2.15, and the core prints can be seen on the wax pattern shown in Fig. 2.16.

The investment casting engineer must also determine how the metal will flow from the runner system to the wax pattern and has to design a feeder connection between the two, which is known as a *gate* (Fig. 2.16). The gate has to allow sufficient metal to flow into the pattern cavity from the runner before it freezes, during solidification of the metal during casting, to reduce the formation of microporosity.

The gate position also affects the grain structure of the casting during solidification, because normally under ambient cooling conditions, the last section to solidify is the hottest position in the system. If this is the gate area, then where it contacts the casting, the grain size will be large, which represents a weaker structure than a fine or equiaxed grain structure. It is therefore important to ensure that the gate position is not at, or in close proximity to, an area of significant high stress in the design, where the highest

FIG. 2.15. View inside a wax pattern tool cavity of an acetabular cup with three ceramic core print locations.

FIG. 2.16. A wax pattern of an acetabular cup showing the gate on the convex surface and three ceramic core prints.

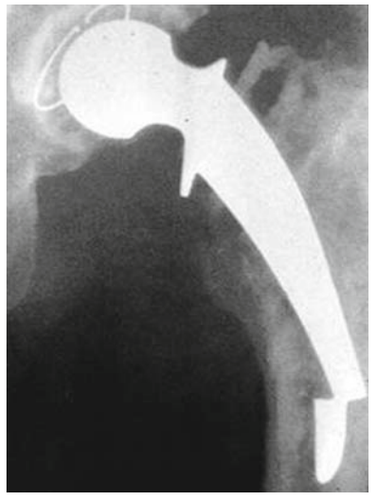

FIG. 2.17. As-cast femoral hip stem showing fracture at the distal third.

FIG. 2.18. Wax injection machine, or press, injecting wax into a wax pattern tool.

fatigue strength in the casting would be required. An example of such a position would be the lower third of a narrow cast femoral stemmed prosthesis, which over time has proved to be the inherent weak point of a femoral stem under the tortional loading at the hip joint. An example of a femoral stem device that failed in its lower distal third because of low fatigue strength properties in the as-cast condition is shown in Fig. 2.17.

As well as identifying the optimal structural position, the engineer must also consider how easily the gate can be removed after casting and how easily the casting profile can be restored. Having identified the gating position on the component design, the engineer can design the wax pattern tool. This tool will contain the cavity of the wax pattern shape and its gate or gate pad if the overall shape is too complex for a simple tool split. The tool has to allow the injection of liquid wax into the cavity and then allow the wax pattern to be removed. The cavity is split, usually along a line of symmetry of the pattern, and this split is replicated in the wax pattern tool. In the case of the Ring prosthesis, the femoral component tool cavity was produced by having half of the medial lateral profile of the stem in each half of the tool. This included approximately half of the femoral head and the fenestrations, or holes, in the proximal stem, which were also produced in each half of the tool. The recess in the femoral head was produced by a sliding metal core, which produced a 2- to 3-mm wall thickness in the femoral head. The two halves of the wax pattern tool were held close together by placing tapered dowels in the corner of the tool to ensure accurate alignment of both cavities in both halves of the tool. Any malpositioning of the tool cavities results in a mismatch between the two halves of the pattern, and there may also be evidence of a die line on the split line position on the pattern. The liquid wax, at temperatures ~60°C to 70°C, is injected into the wax pattern tool through a small-diameter hole in the side of the tool (Fig. 2.18) and is usually routed through a sprue to the wax pattern gate.

This allows the wax sprue to be removed without significant damage to the wax pattern. As the lost wax, investment casting process is capable of faithfully producing the features on the wax pattern, a thorough inspection and repair of the wax patterns takes place prior to further processing.

Before I explain the next stage of the investment casting process, it is necessary to be aware that the wax pattern is approximately 2% larger than the required final metal casting as there are a number of expansions and contractions that take place throughout this process. The first contraction experienced is when the liquid wax is injected into the tool cavity and the warm wax contacts the cooler metal tool. This contraction is of the order 0.5% but is dependent upon the actual process parameters at the foundry and upon the specific geometry and section thickness of the component. Clearly, a thinner section thickness will solidify faster than will a thicker section and therefore maintain its injected size. Also, complex geometries will restrict certain contractions due to solid metal tooling inserts, such as the fenestrations on the Ring prosthesis.

After the inspection of the wax patterns, they are assembled onto a wax runner system by welding them to the runner by melting the gate using hot pallet knives or gas flames. The wax runner is a wax tree where the branches are connected to a funnel that eventually forms a pour cup to allow liquid metal to enter the ceramic mold (shell) cavity. It is imperative that the junction between the gate and the runner is sealed to prevent the penetration of liquid ceramic into the wax assembly, which occurs at a later stage in the process. The wax patterns are arranged on an appropriately designed runner system to ensure that they are close enough to allow an economic mold size, but separated sufficiently to ensure that they do not insulate each other during cooling after metal casting to affect the required microstructure. In the inside of the wax pour cup, there is a nut that has been secured in place by producing, or injecting, the wax runner system around the nut, in much the same way as the wax pattern is produced. Once the wax assembly is complete, the mold can be transferred to the shelling, or investment, area.

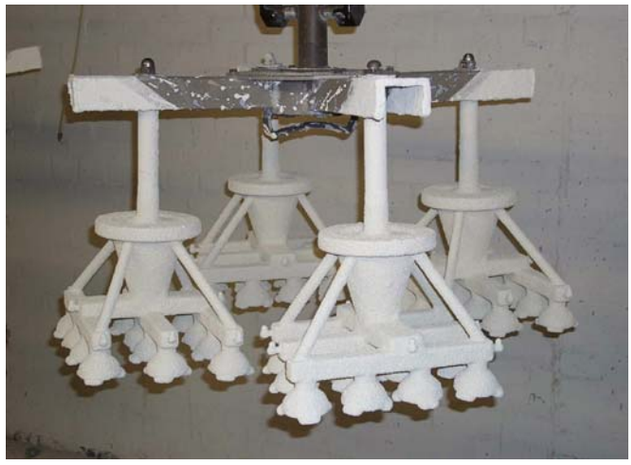

FIG. 2.19. Wax assemblies supported by a robotic arm for shelling.

A metal pole is screwed into the nut in the wax pour cup, which allows the mold to be manipulated by an operator. Historically, the shelling process was a manual operation. More recently, robotic systems have been introduced that provide more consistency and greater mold size and economies of scale to be enjoyed (Fig. 2.19). Ceramic shell molds are made up of three components: the binder, the filler, and the stucco materials. The binders are usually made with silica, a ceramic material, and are either water or alcohol based. Filler and stucco materials are used in a wide range of combinations including silica sand, alumino-silicates, alumina and zirconium silicates. The process of shelling, or investing, the wax assembly involves immersing the mold into liquid ceramic and then applying a coat of solid ceramic, or stucco, onto the liquid layer.

Each coating is allowed to dry before applying the subsequent coat, and the process continues until the shell coating is approximately 4- to 5-mm thick all over the wax mold. The first coat is critical for achieving fine detail on a casting surface and can influence the resultant grain structure of the casting if any grain nucleation additions are made to the coating. It has been demonstrated that additions of cobalt aluminate in the first coat, or face coat, can initiate grain growth when the CoCr alloy meets the shell surface, resulting in a finer grain size and structure than would otherwise result. This can be useful if high fatigue strength properties are required on the final casting. The subsequent coats, which can be 10 or more further coats, have coarser textures and are used to develop a harder, stronger shell. The time between shell coatings is dependent upon the specific parameters specified by the foundry producing the components. A typical drying time for each coat is of the order 4 hours with a total shelling time of 2 to 3 days. When the final seal coat is applied, there is no stucco applied to the surface, which allows the final coat to be of a smooth texture sealing the ceramic particulates on the surface.

The shells, still containing wax assemblies, are moved to the dewaxing process where, inside an autoclave, they are subjected to steam temperatures of 150°C to 180°C. At this temperature, the wax melts and drains from the opening of the pour cup leaving an empty shell with residual wax on the shell surface. Vents are designed on the runner system to allow wax to escape from the patterns and runner system to reduce the risk of cracking the shell due to the differential in thermal expansion between the wax and the shell materials. After dewaxing, the shells are flash-fired in a gas-fired oven to burn the residual wax, leaving the shell clean and empty (Fig. 2.20). Careful selection of waxes with low ash contents are used to reduce the risk of residual impurities remaining in the shell. A thorough inspection of the shell takes place to identify any cracks and vents that require repairing, using a refractory cement to seal the shell prior to the casting process. It is important to ensure that there are no impurities inside the shell cavity prior to casting as these may become inclusions in the metal once the casting process commences. In contemporary practice, a refractory filter is fitted to the mold mouth to allow a filtering of inclusions that may be carried over in the molten metal. This process was unlikely to have occurred during the manufacturing of the first-generation metal on metal bearings.

The inspected shell is placed into a gas-fired preheat furnace where it is soaked at a temperature of ~1050° C for an hour or more (Figs. 2.21 and 2.22).

FIG. 2.20. Ceramic shell after dewaxing and flash-firing.

FIG. 2.21. Preheat furnace.

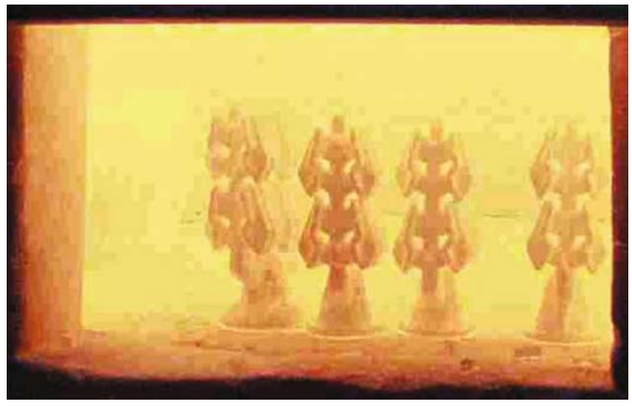

FIG. 2.22. Molds at temperature (~1000°C) in preheat furnace.

The temperature of the preheat process is generally above 1000°C where the ceramic material is sintered and undergoes a phase change from its green state and is rendered inert to the molten metal that will be poured into the shell. While the shell is being preheated, a billet of CoCr alloy, cut to the required weight, is being melted in an induction furnace in a preformed refractory crucible. As the CoCr alloy contains highly reactive elements such as titanium, it is important to protect the metal from oxygen in the atmosphere by melting under an inert gas atmosphere or in a vacuum chamber. Once the alloy reaches the foundry-specified temperature, usually above 1550°C, which is measured in real-time using a thermocouple, the shell is taken from the preheat furnace and placed upside down, so that the pour cup is like a funnel, in the casting furnace. In the case of a vacuum furnace, the mold is placed in a mold chamber, which can be evacuated prior to entering the casting chamber, and in the case of an inert gas cover rollover process, the mold is placed above the molten metal. When the shell is adequately protected, in either process, the metal is transferred to the shell by pouring the liquid metal (see Fig. 2.23). This process takes a few seconds, and the shell, full of metal, can be removed from

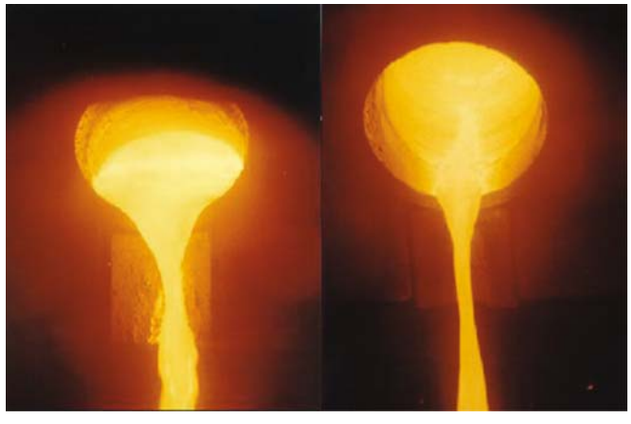

FIG. 2.23. (A, B) Molten metal pouring from the crucible (~1560°C).

FIG. 2.24. Molds on foundry cooling rack after casting.

the casting stage and placed on a foundry rack and allowed to cool (Fig. 2.24).

It is during this cooling process that the microstructure of the casting will form. As the metal is at a much higher temperature than is the shell (1550°C compared with 1000°C), cooling starts at the surface of the shell-metal interface.

Nucleation of grains starts by the precipitation of dendrite arms that grow, like Christmas trees, into the liquid metal (Fig. 2.25).

The solidification process starts at the liquidus temperature (~1395°C for CoCr alloy) and finishes when the solidus temperature (~1230°C for CoCr alloy) is reached. The liquidus and solidus temperatures vary with subtle differences in chemical composition of the alloy and are often only applicable in what is called *equilibrium* conditions where environmental cooling influences are reduced. The dendrite structures are predominately rich in the higher melting point elements and can be seen as *coring* in the as-cast microstructure. As

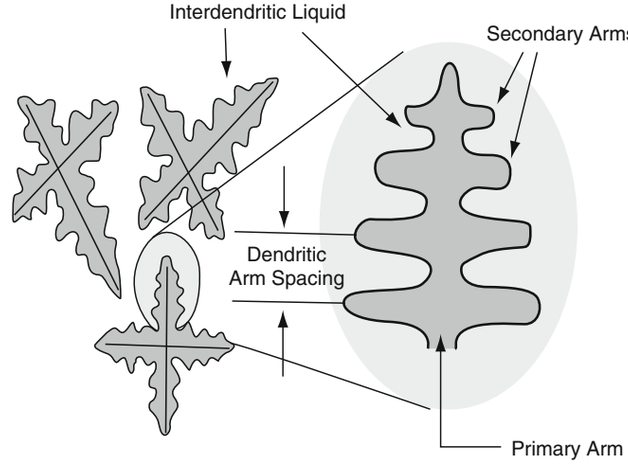

FIG. 2.25. Dendritic pattern formed during the solidification from liquid metal.

the total system continues to cool and the dendrite arms continue to grow, the solid phase dominates the volume in the mold cavity, and the residual liquid between the dendrite structures is rich in the lower melting point elements. When these residuals solidify, they form predominately as the interdendritic carbide phase, rich in chromium, molybdenum, and carbon, and form in the Chinese script morphology previously described. Upon complete solidification, the metal component has contracted from the shell cavity size to a size approximately 2% smaller than the starting wax pattern.

The shell material cracks during the final cooling process and is removed using a short vibratory process followed by blasting the casting surface using stainless steel shot where the surface texture permits. Once the connecting gate between the casting and the runner can be clearly seen, the individual castings can be removed using rotating cutting wheels or gas cutting techniques. In all cases, great care is taken to avoid damaging the castings as repair by welding is usually not permitted in the case of medical devices. Once separated from the runner, each casting can have its gate reduced in size, or formed to the casting profile. Traceability of each casting to its respective manufacturing history is maintained, and vibroetching can be used to permanently identify the castings.

The metal castings can be inspected to specified criteria and can include visual, gauging, fluorescent penetrant (crack detection), and radiographic inspection methods. Rejected castings and residual runner system alloy pieces are reverted into new billets for future casting production. Metallurgical examination can also be carried out by macro grain etching the casting surface to reveal the grain structure or sectioning and etching to reveal grain boundaries and metallurgical phases in the microstructure.

Thermal Treatments of Cast Alloys

As described earlier in this chapter, the McMinn metal on metal resurfacing hip raw-material castings had been produced in the as-cast (not heat treated) microstructural condition and/or subjected to variable thermal treatments, including SHT, HIP, and both SHT and HIP conditions (Fig. 2.1). The reason for employing these treatments was to reduce and/or remove microporosity from the microstructure when HIP is employed and to homogenize the microstructure to reduce residual casting stresses when SHT is employed. Annealing the material at temperatures below the eutectic temperature of the alloy prevents the carbides from melting and produces an equalization of the dendritic segregation, without the loss of tensile properties. This process is normally carried out at temperatures around 1170°C. HIP was introduced in the 1980s as a method of improving the fatigue strength properties of alloys used to produce components for the aerospace industry where complex shapes and light weights were commonplace, putting high demands on the alloys employed. Cobalt-containing alloys have been extensively used in the aerospace industry since the 1930s by the Austenal Company (Warsaw, IN). This helped to develop a better understanding of the complex metallurgical transformations that can occur in these alloys and facilitated their later usage in medical grade applications.

The typical process for thermally heat treating CoCr castings is to preheat a gas-fired furnace to the required temperature and then to load the castings in an appropriate formation on racking, dependent upon the size of each casting and the number to be processed together. For medical device–size castings, it is not uncommon for several hundred to be processed at the same time. These can of course be different devices but produced from the same alloy type. The furnace types vary between suppliers of the process. An image of a contemporary furnace can be seen in Fig. 2.26. As can be seen, the furnace volume is approximately 1.5 m × 2 m × 1.5 m.

As the thermal processes are time, temperature, and furnace position dependent, all of which have their own process tolerances, the variation in the resultant microstructures can be extensive.

The typical parameters used for the HIP process of cast CoCrMo alloy are 1200°C for 4 hours in an inert atmosphere followed by a gas fan quench at a relatively slow cooling rate. This thermal treatment is carried out at a high pressure of 103 MPa, which is sufficient to squeeze the micropores out of the microstructure provided that they are not connected to the casting surface. The reason for this relatively slow cooling process is to avoid significant damage to the refractory lining due to the expansion and contraction of the refractory bricks in the furnace walls, floors, and ceilings. The resultant effect on the microstructure is that at this time and temperature, there is sufficient time for the metallurgical phases in the microstructure (carbide precipitates and matrix) to reach a temperature close enough to the solidus temperature (~1230°C)—which is the temperature at which the solid metal starts to melt and become a liquid phase—to start a diffusion process and movement of

FIG. 2.26. Contemporary heat treatment furnace.

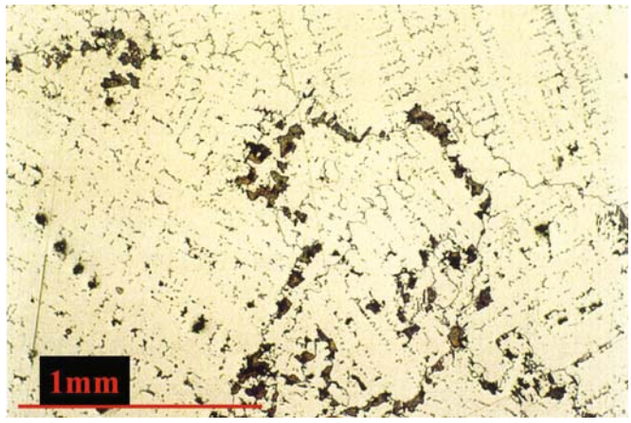

FIG. 2.27. Microstructure of hot isostatic pressed CoCr showing lamellar carbide at grain boundaries.

atoms within the microstructure. At this process temperature, there is a diffusion of the chromium, molybdenum, and carbon atoms from the carbide precipitate into the surrounding face-centered-cubic lattice of the matrix, in the case of Cr and Mo, and into the interstitial spaces in the lattice, in the case of C. As the alloy cools from the process temperature, there is an opportunity for reprecipitation of the carbides. However, they form predominately at the grain boundaries and are not re-formed as the original as-cast morphology. The marked effect that this has on the carbides is that they are reduced in overall size from the "blocky" Chinese script form to smaller, fine, agglomerate carbides that have a lower mechanical stability in the supporting matrix, whereas the matrix itself has larger intercarbide areas, the effect of which will be discussed later. There is also evidence of the formation of lamellar carbides, which are lineated in pattern and found at the grain boundaries (Fig. 2.27).

In this microstructural condition, the mechanical properties of the alloy are generally below those required by ISO 5832 part 4 (Table 2.3), and subsequent treatments, such as SHT, are employed, where a faster quenching rate can be achieved to restore the required mechanical properties. After the reduction in carbide, grain size can increase due to the reduction in grain boundary pinning, which is enjoyed by the presence of grain boundary carbides. This also increases the ductility of the material. The subsequent heat treatments that follow HIP do not further influence the microporosity but can significantly alter the already modified carbides.

TABLE 2.3. Mechanical properties

Tensile strength	Proof stress of nonproportional elongation	Percentage elongation after fracture[1]
R_m	$R_{p0,2}$	A
min.	min.	min.
MPa	MPa	
665	450	8

[1] Gauge length = 5,65 $\sqrt{S_o}$ or 50 mm, where S_o is the original cross-sectional area, in square millimetres.

The typical parameters used for the SHT process of cast CoCrMo alloy are 1200°C for 4 hours in an inert atmosphere followed by a rapid gas fan quench to 800°C in less than 8 minutes (50°C per minute). Unlike the HIP process, there is no requirement for a significant pressure in the chamber other than to maintain an inert gas atmosphere to prevent oxidation of the castings due to the reaction with oxygen at temperature. This is achieved by heating in a vacuum chamber. The inert gases used are typically argon or nitrogen and partial pressures of 2.7 to 5.3 mbar. As the temperature is similar to that employed in the HIP process, the effect on the carbides is to continue their diffusion into the matrix. With the rapid gas fan quench cooling, their reprecipitation is restricted, resulting in much of the carbide remaining in the matrix solution. When a CoCr alloy casting has been heat treated and its carbide morphology altered, further subsequent heat treatments diffuse the remaining carbides at a more significant rate. This results in a dramatic reduction in the phase proportion (volume fraction) of the carbide phase in the matrix. The measurement of the amount of carbide present in a microstructure is carried out by identifying a field of interest and capturing it on a micrograph at an appropriate magnification. Using imaging analysis techniques (e.g., Image Pro Plus), it is possible to identify the carbide phase by its contrast against the matrix on optical or SEM images (Figs. 2.28 and 2.29).

These identified contrast areas are then calculated as a percentage against the total *field of view* area.

The significant effect on the carbide morphology after a single thermal treatment of 1200°C for 4 hours can be seen in Fig. 2.30, where the phase proportion has been halved. It can be seen at this higher magnification that the diffusion of chromium and molybdenum from the carbide results in the stable block morphology being transformed into a fine, dispersed morphology, which is less mechanically stable and exposes more area of the matrix.

The reducing amount of carbide phase observed after a single thermal heat treatment over time is expressed as the Larson-Miller parameter (Fig. 2.31). As can be seen, the higher the temperature and the longer the time at which the casting is exposed to the temperature, the more significant the reduction in carbide phase becomes.

Therefore, if a CoCr casting is exposed to multiple thermal heat treatments at the solutionizing temperatures, the resultant microstructures will have small, fine, dispersed carbides with a low carbide phase proportion and more surface area of the matrix exposed as seen in Fig. 2.30. The significance of these modifications is that the finer dispersed carbides are less mechanically stable within the supporting matrix, because they are smaller and more easily extracted during articulation against another surface, and that the larger areas of matrix exposed are at a higher risk of adhesive wear against the counterface of the bearing. I have previously mentioned a number of studies that show the significance of the carbide phase and its resistance to wear [2–7]. However, it is interesting to consider that a number of other studies have

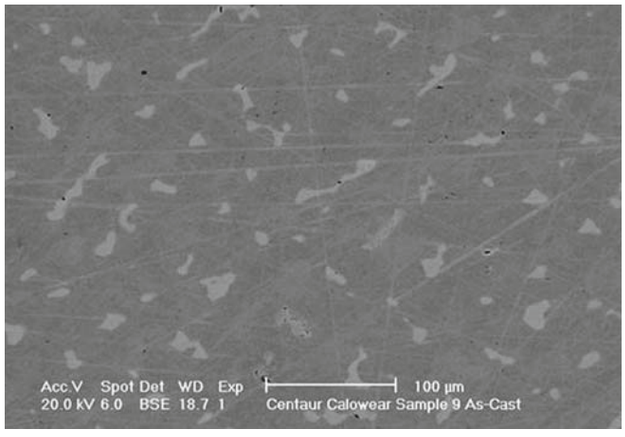

A

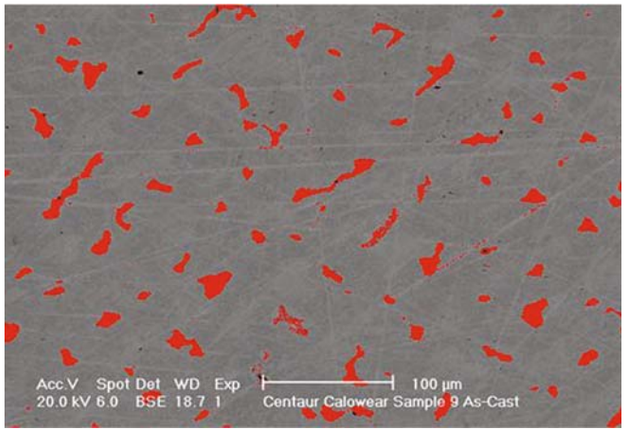

B

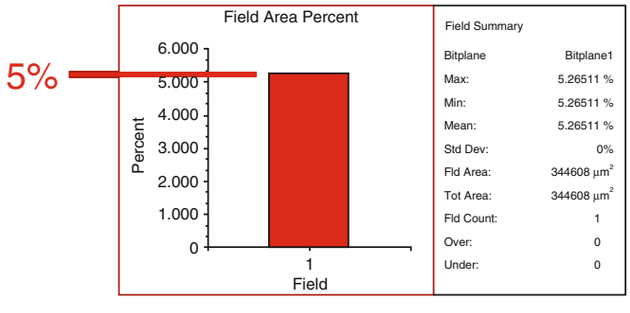

C

FIG. 2.28. Image analysis used to quantify the carbide phase in the field of view in an as-cast microstructure.

failed to identify the relationship between the reduction in carbides in the microstructure and the wear rate of the bearings. This is most probably because, during hip simulator studies, the articulating surfaces are protected by the generation of a fluid film as the components are both optimally positioned in relation to one another and that they are in continuous motion promoting the entrainment of fluid. When CoCr materials are tested for their wear resistance using pin on plate or pin on disk methods, there is a statistically significant difference identified in the wear properties with the as-cast, block carbide having the lowest wear. The subject of wear testing and results are described later in this book.

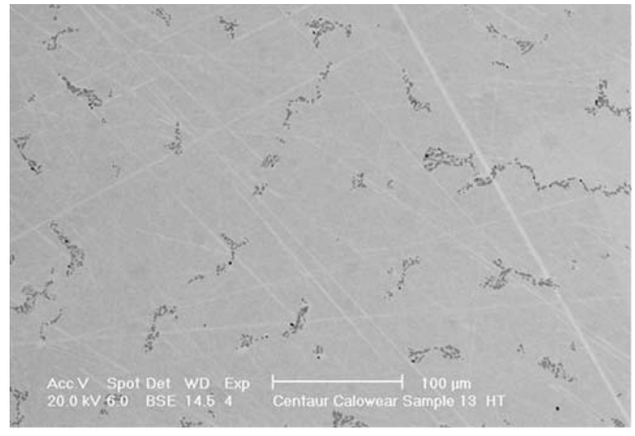

A

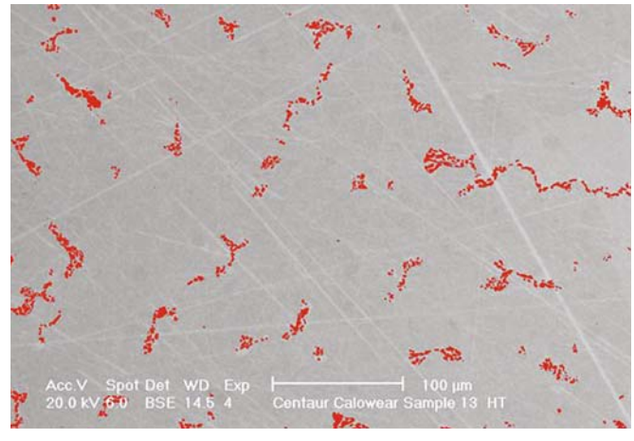

B

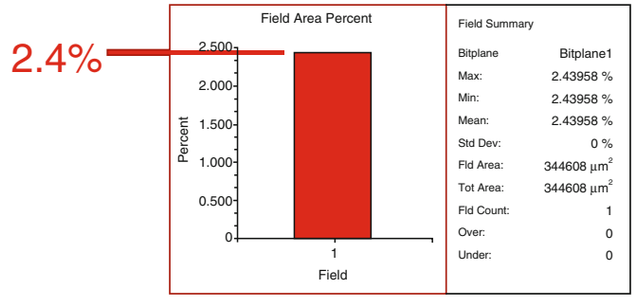

C

FIG. 2.29. Image analysis used to quantify the carbide phase in the field of view in a heat-treated microstructure. After a single heat treatment, the phase proportion is reduced by 50%.

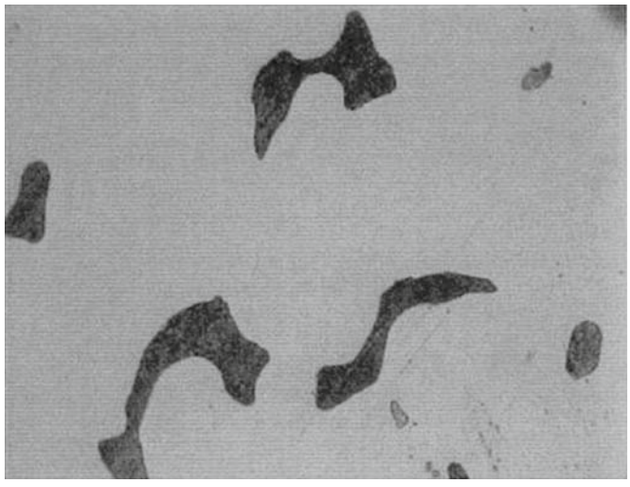

A

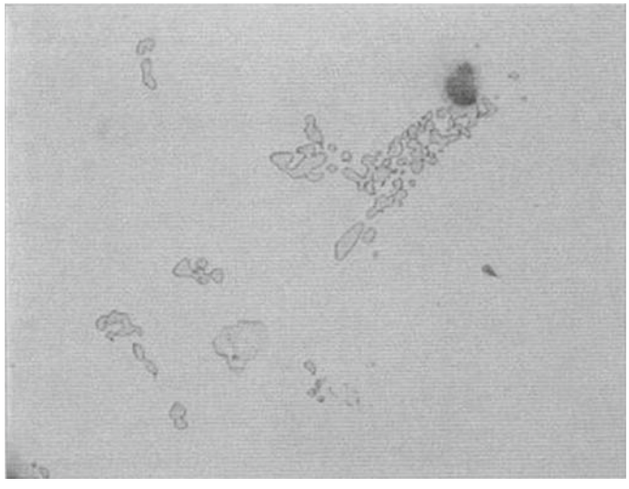

B

FIG. 2.30. (A) High magnification of carbide phase in the as-cast block and (B) fine dispersed, particulate, morphology after a single thermal treatment at 1170°C for 4 hours.

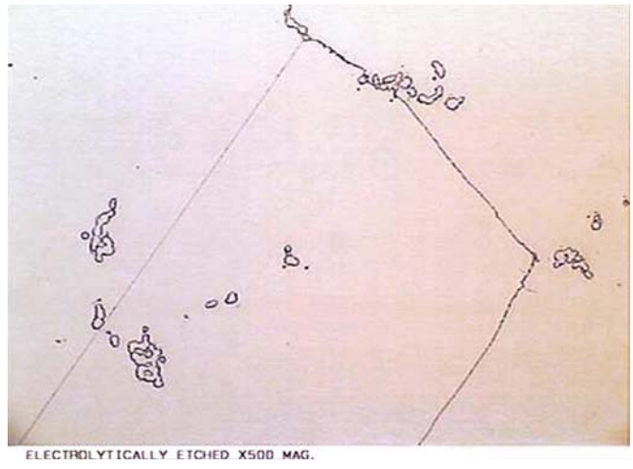

FIG. 2.32. CoCr cast alloy after HIP and SHT.

Other examples of contemporary metal on metal bearings are shown in Figs. 2.32 and 2.33 where essentially a material containing high carbon (>0.2%) with the same bulk chemistry has been subjected to post-cast thermal treatments and the carbide structure has been disintegrated.

As well as the previously described thermal treatments, other processes such as sintering, by which beads are attached to the convex surface of an acetabular cup device, are employed in the production of some orthopedic devices. This high-temperature process also modifies the microstructure through a diffusion process of the carbides. Another point worthy of mention is that these thermal treatments were not used in the first-generation metal on metal bearings, and therefore there is no long-term clinical experience to complement their use.

The reduction in carbide size and the exposure of matrix surfaces subject these structures to a significant risk of adhesive wear when matrix contact occurs in the bearing between the articulating surfaces. The distraction of the smaller carbides from the supporting matrix occurs more easily when compared with the as-cast microstructure.

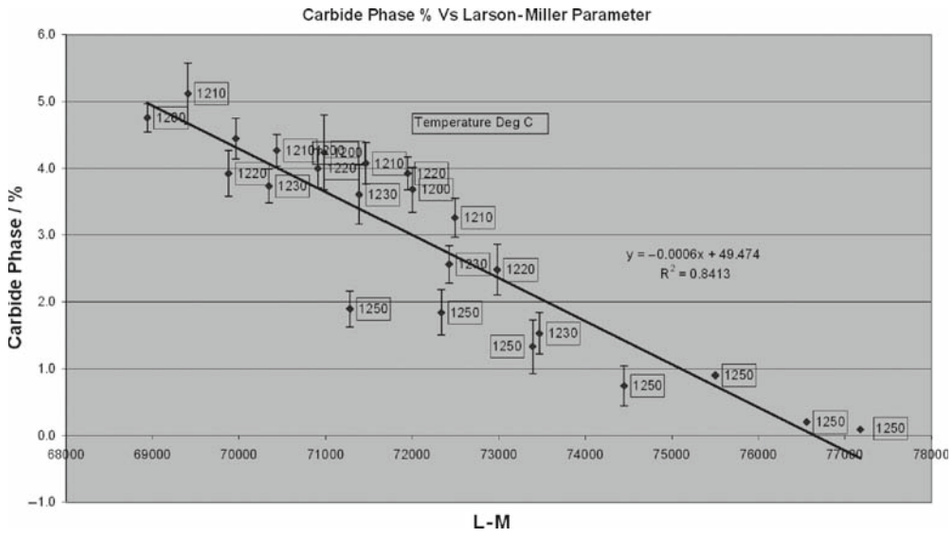

FIG. 2.31. Carbide phase % versus Larson-Miller parameter.

FIG. 2.33. CoCr cast alloy after sintering, HIP and SHT.

The Development of the Birmingham Hip Resurfacing Device

When I first met Derek McMinn in 1995, I was the proud owner of a full head of hair. After my involvement in the transfer of the McMinn metal on metal resurfacing from Trucast to Centaur, which has been described earlier, I was involved in the development of the Birmingham Hip Resurfacing (BHR) device. My initial task was to characterize the metallurgical features of the first-generation metal on metal devices and to establish a bearing material specification based on these characteristics, which led to the long-term clinical success of the CoCr metal on metal bearings. This, as previously described, was to specify the BHR in CoCrMo alloy to ISO 5832 part 4 chemistry in the high carbon grade and in the as-cast microstructural condition. The objective was to employ state-of-the-art foundry practices and to replicate the coarse block carbide morphology in the as-cast condition. Without the benefit of employing the HIP process to reduce any casting voids, or microporosity, the gating design of both the femoral and acetabular components required efficient feeding capabilities.

I was also tasked with the development of an integrally cast surface texture on the convex surface of the acetabular cup to negate the need for any thermal processes to attach a porous surface, which would significantly modify the as-cast microstructure. Derek McMinn was dogmatic and adamant about this due to his previous unsatisfactory experience with the McMinn resurfacing device. It was this part of the project that made the highest demands and brings back the most memories of late nights, pondering, and hard work. The development of this surface included many late-night meetings with Derek, where I listened to numerous descriptions of what the "ideal" surface texture would look like. I also need to add the fact that none of them was capable of being produced through the conventional wax pattern tooling methods, which was due to the fact that the surface texture was to be produced as an undercut feature to produce a mechanical interlock for the resultant bone on-growth. Derek made many "visits" to the foundry in Sheffield. Initially, his aim was to learn everything about cobalt chrome and the casting process. He then started to get his hands dirty by joining workers on the factory floor in every stage of the casting process. We had never before seen a surgeon with this level of interest. None of us had the heart to tell him that everything he touched had to be scrapped as he was "untrained"! It must also be stated that cobalt chrome alloy has not proven itself to be an effective osseo-integrating material, unlike titanium alloys.

Mr. McMinn's preference was to have a beaded surface texture with a defined bead spacing to permit adequately sized pedestals of bone to grow between and underneath the equator of the beads under the positive influence of hydroxyapatite. Our intention was to stick a suitable material to the outside of the blank wax pattern surface, which could then be invested in the shelling process. I wanted to see if wax beads could be produced in 1-mm-diameter spheres by dripping molten wax into cold water, but this idea was met with great despair at the foundry. I was later informed, by reputable and reliable sources at Centaur, that there was no such medium available that would allow such a surface to be produced.

My meetings with Mr. McMinn identified a number of other bead-shaped mediums such as icing sugar decorative beads and even poppy seeds! These were trialed by sticking them to wax patterns with large flat surfaces or other shapes (Fig. 2.34), but their shortcomings were soon identified if they were either soluble, in the case of sugar-based materials, or absorbent and explosive, in the case of poppy seeds, when they were immersed in the investment slurries or fired off in the flash-fire furnaces.

The resultant cast surfaces were far from optimal. Other suggestions included intricate structures produced by sprinkling

FIG. 2.34. Wax pattern covered in poppy seeds.

FIG. 2.35. Wax pattern covered in decorative glitter.

decorative glitter particles or even tea leaves onto the surfaces of waxes to test the resultant cast surfaces (Figs. 2.35 and 2.36).

This iterative process of "design, try, and test" became a regular activity, and it is worthy of note that I was delighted to receive the support of Dave Skupien, Bob Bruce, and the late John Harris, who were part of the Centaur management, in the pursuit of a final objective. One particular incident that left me with a real problem was when Derek convinced me that we were on the edge of identifying the final surface texture, which involved the use of tea leaves from Harrods tea, blend 20. How on earth would I be able to get hold of Harrods tea leaves in South Yorkshire? Anyway, we continued to produce a number of wax patterns covered in Harrods tea leaves, and I persuaded colleagues in the operations department at Centaur to process these components only to find that the isoferulic acid in the tea leaves reacted with the ceramic slurry resulting in the contamination, discoloration, and wastage of an expensive slurry. Imagine, a casting engineer not knowing that! The resultant surface texture was actually not too bad, however. We had even considered building a metal *master* that could be used to produce a rubber mold to place inside the wax pattern tool, injected with wax, and then peeled off the surface, but this was beyond our development timescale.

It was by pure coincidence that I was visiting another business contact at the Casting Technologies Institute (CTI) in Sheffield, where they operate a polystyrene pattern casting process, that I stumbled upon large volumes of polystyrene beads of roughly 1 mm in diameter. These beads, it turned out, were the pre-expanded beads used to produce the polystyrene patterns in the CTI casting process. I couldn't wait to return to my own process with a container full of these beads and "test" how they might perform under the Centaur casting process. Finally, we had a breakthrough in our development program, and these beads produced a surface texture exactly as Mr. McMinn had originally requested (Fig. 2.37).

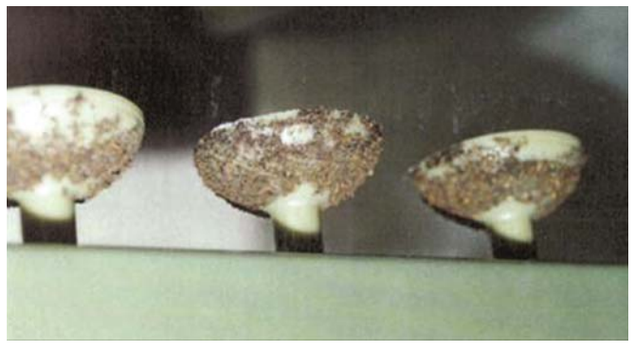

FIG. 2.36. Wax pattern covered in tea leaves on a wax runner.

There was of course a whole series of other process issues to overcome, but we had finally identified a suitable material for what was to become trademarked as Porocast.

To complement the polystyrene beaded surface, it was necessary to develop a bonding technique and a leachable face coat to invest this undercut surface (Fig. 2.38).

The bonding technique is not discussed here, and my only reference is to the adoption of a primary investment coating that has a capability of being leached by an alkali solution, a number of which are available to investment casting foundries with a design need. As the standard method of shell removal, blasting, is a line-of-sight process, it is not capable of removing the face coat from under the beaded texture, and so an effective chemical process is required to remove the residual shell. Just

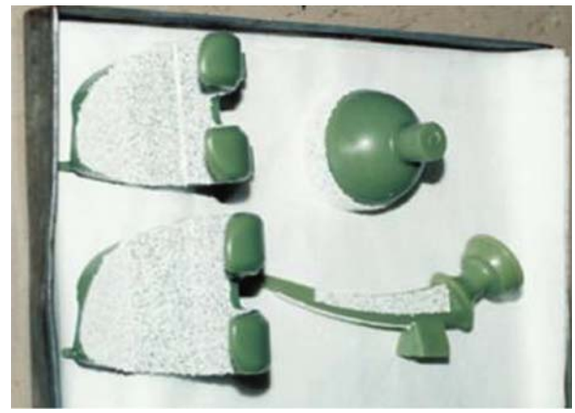

A

B

FIG. 2.37. (A) Wax patterns covered in polystyrene beads; (B) the resultant cast surface.

FIG. 2.38. A section of a shell showing the detail of the Porocast structure.

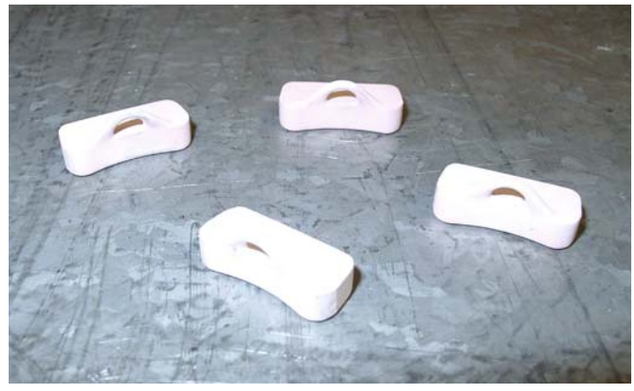

FIG. 2.40. Ceramic core used to produce the cast in introducer threaded wormholes.

as the leachable face coat processes are widely available to the casting community, so are the chemical leaching processes.

The third development activity for the BHR acetabular component casting was to produce the tunnels, or wormholes, which allow the threading of the introducer wires into the thin wall section of the casting on the face of the cup. The use of ceramic cores to produce detailed features in a CoCr casting was not new to Centaur as previous developments had included producing a ceramic core with a detailed M8 thread that reduced significant time, difficulty, and cost in the finish machining of a femoral knee device (Fig. 2.39).

This allowed for the attachment of augmentation blocks on the inner surface of the knee component. As that particular ceramic core was performing well, it appeared logical to use that ceramic material type to produce a ceramic core capable of producing the 1.75-mm-diameter holes in the BHR cup for threading the introducer wires through. The critical aspect of the ceramic core for this feature was that the threaded hole needed to match the radius of the cup peripheral face, dictated by the radius and the wall thickness, match the curvature of the cup, dictated by the external and internal radii, and for one ceramic core to complement each size of cup. Another small challenge! A small team of engineers from Centaur, Finsbury (Leatherhead, UK), and Certech (Kettering, UK) (ceramic core suppliers) worked on the final design, which ended up looking like a small stirrup (Fig. 2.40). The resultant ceramic core allowed an optimal position for the wormhole, or tunnel, so that the cavity was central to the casting section in all planes.

The development of the femoral head casting was rather less challenging than that of the acetabular cup as its external surface was to be extensively machined, which means that a gating design could take advantage of that activity. The gate therefore was positioned centrally on the zenith of the head sphere and was large enough in diameter to effectively feed the casting without microporosity. An inner core was produced

A

B

FIG. 2.39. (A) Ceramic core used to produce an M8 thread in a femoral knee; (B) cross section of the resultant cast form.

FIG. 2.41. The internal detail of the femoral head casting produced on the casting without machining.

in the wax pattern tool to create the internal profile, stem, and cement pockets (Fig. 2.41).

Once the casting process was determined, which included the design of the wax pattern and gating, the wax assembly, shelling technique, casting technique, finishing methods, and inspection methods, the casting validation process took place. Initially, we employed bizarre logistical processes that included the transportation of wax assemblies across South Yorkshire for the shell investment to take place at a development site, while Centaur was developing an in-house leachable face coat. More hair loss! The final casting process was effectively validated and locked down to ensure continued compliance with the product specification, and all characteristics of the castings met with Mr. McMinn's expectations. We had produced a casting system that replicated the excellent material properties of the first-generation metal on metal bearings with an integrally cast in-growth structure and an efficient introducer system that allowed a thin wall casting section cup to be gripped without encroaching on the important articulation surface of the bearing (Figs. 2.42 and 2.43).

Summary

In the preceding sections, I have covered the forensic analysis of successful long-term retrieved metal on metal implants, detailed descriptions of a number of manufacturing and technical processes, the development of the BHR device, and microstructural changes in CoCr alloy due to thermal processes and its subsequent effect on wear. I will summarize this chapter in the following section bringing the salient points together from each of the topics covered to establish their combined significance.

A

B

FIG. 2.42. (A) BHR cup with Porocast surface; (B) high magnification of beaded surface.

The critical factors that had provided such an excellent performance in the first-generation metal on metal bearings were that the CoCr microstructure was produced in its highest wear-resistant condition, with large block carbides protecting the metal surfaces from adhesive wear (Figure 2.30A), both articulating surfaces were similar, reducing the risk of having a subservient component and articulating pair, and the manufactured geometry resulted in sphericities and clearances that would allow at least partial fluid film to occur during articulation of the bearing. As the fatigue strength failures of long-stemmed devices did not occur until later in the implants (fatigue is a cyclic effect on a structure that involves elastic or plastic bending or movement over time and under load), the use of as-cast microstructural condition was fortuitous for the bearing properties of the material and allowed the experience of CoCr as a metal on metal bearing to continue.

The McMinn metal on metal resurfacing device was produced and implanted between 1994 and 1996, and part of its material, microstructural evolution has already been described in detail. The significance of this device is that the product

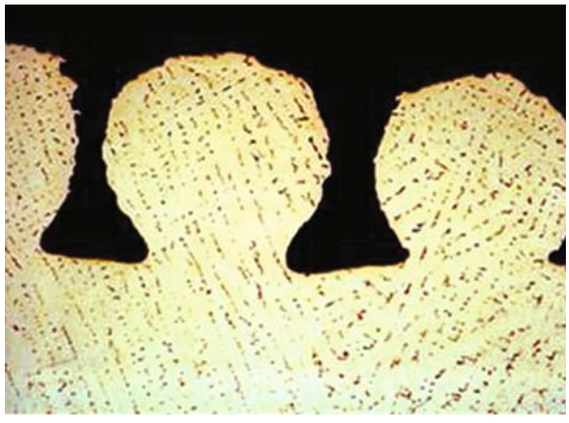

A

B

FIG. 2.43. (A) Cross section through Porocast beads; (B) high magnification of cross section through a single bead.

produced in 1996 had a microstructure that was based on high fatigue strength, high manufacturing yield (no scrap due to casting microporosity), and easiest machining condition (Fig. 2.32 as an example) and has behaved differently than those devices produced and implanted in 1994 and 1995. The microstructure generally had small dispersed carbides and large areas of matrix exposed between the carbides, however due to the variability in thermal treatments, evidence on some retrievals from this group show a higher diffusion of carbide. Of course, there are a number of causes of implant failure, septic or aseptic, which result in the need for revision, and when investigating a revision it is important to determine what role the implant materials and or design have played in the cause. The details of the implant cohorts, including revision rates and causes of revision, are described by other authors in this book.

The microstructures of the retrieved devices from the McMinn cohorts implanted in 1994–1996 were examined to determine if there was any relationship between the material of the device and the cause of revision (i.e., metallosis-induced osteolysis). Because the product implanted was taken from implant stocks (including finished goods, work-in-progress and casting stock), it appears that products implanted in 1996 included products that were produced in 1995, or earlier, leading to combinations of microstructures articulating against each other and artificially increasing the cohort size for 1996, therefore understating the revision rate. It was interesting to see in those devices revised for metallosis-induced osteolysis that there was a direct relationship between the microstructure of the device and the linear wear rate measured, where low-carbide-containing devices had higher wear when both bearing surfaces were in parity. It can also be seen that the higher-carbide-containing microstructure protects the device from the counterface, which becomes subservient, whether it is a femoral head or an acetabular cup component. This is in contrast with the previously reported observation that the linear wear rate of the femoral component is higher than that of the acetabular component when the microstructures are in parity (e.g., first-generation metal on metal bearings and BHR). Of course, if the femoral device is protected by being produced in a higher-carbide-containing microstructure, the total wear of the bearing will be lower than when both surfaces are low carbide as it is the linear wear of the head that is most easily identified due to the localized position of the smaller wear patch and ease of measurement of a convex object.

The lower-carbide-containing alloy (carbon <0.07%) microstructures have a greater risk of experiencing adhesive wear on asperities in the matrix on both bearing surfaces, which occurs at a nanometric level, than do the higher-carbide-containing bearings where the large block carbides, because of their higher hardness, reduce the occurrence of adhesive wear. It is the biphasic nature of the hard carbides in the softer matrix that provides the CoCr alloy with its excellent wear properties. I remember attending an excellent seminar on "Tribology in Practice" at the National Physical Laboratory in the United Kingdom, where it was described by Neale and Gee that "for loaded metal-on-metal contacts some lubrication is essential to avoid seizure and wear. The optimum structure is then one in which there are small dispersed hard areas in the surface to carry the load, supported in a strong but softer matrix, which wears to form recesses around the hard areas, and in which lubricant can be retained. In the case of piston rings and cylinder liners which are made from cast iron, this is achieved by adding phosphorus, vanadium to chromium to create localized hard areas of phosphate or metal carbides." It occurred to me that it was serendipity that the as-cast CoCr microstructures produced for the first-generation metal on metal bearings had an inherent protection to adhesive wear, due to these large block carbides, and had allowed these bearings to perform. Low-carbide-containing bearing surfaces, where high material loss had been experienced, evidenced adhesive wear when their articulating surfaces were scratch-free and did not have particulate available (i.e., carbide particulate) for abrasive third-body wear scratches to form.

Although there are other design factors that can contribute to the failure of a metal on metal bearing device, the material condition is of fundamental importance to the longevity of these devices, which are intended to be *in situ* for many decades, and there are already reports, both written and anecdotal, suggesting that the use of mixed microstructures or low-carbide-containing bearings are leading to early failure of these devices [8–14]. The use of low-carbon alloys, which do not have sufficient carbon to produce carbides and where there is no inherent protection against adhesive wear, are no longer used for metal on metal bearings, however high-carbon-containing alloys that have been thermally treated, reducing the carbide content and behaving like low-carbon alloys, continue to be used. The problem with the risk of high wear in the bearing material due to microstructural differences in the *in vivo* situation (i.e., in the patient and outside the laboratory) is that it does not manifest itself until the midterm time period. Any bearing material wear risks must be considered as latent risks and should be a consideration when choosing a bearing material for use in orthopedics.

References

1. Medley J et al. Engineering issues and wear performance of metal on metal hip implants. 1997.
2. Ahier S, Ginsburg K. Influence of carbide distribution on the wear and friction of Vitallium. Proc Inst Mech Eng 1966;181:137–139.
3. Clemow AJT, Daniell BL. The influence of microstructure on the adhesive wear resistance of a Co-Cr-Mo alloy. Wear 1980;61:219–231.
4. Wang KK, Wang A, Gustavson LJ. Metal on metal wear testing of chrome cobalt alloys. In: Digesi JA, Kennedy RL, Pillar R, eds. Cobalt-Based Alloys for Bio-Medical Applications. ASTM STP 1365: Wear Characterization. West Conshohocken, PA: ASTM, 1999:135–144.
5. Que L. Effect of heat treatments on the microstructure, hardness and wear resistance of the as-cast and forged Cobalt-chromium implant alloys. Presented at the Symposium on Cobalt-Based Alloys for Bio-Medical Applications, November 3–4, 1998, Norfolk, Virginia, USA.
6. Varano R, Bobyn JD, Medley JB, Yue S. Does alloy heat treatment influence metal-on-metal wear? Poster no. 1399 presented at the 49th Annual Meeting of the Orthopaedic Research Society, New Orleans, Louisiana, USA; 2003.
7. Cawley J, Metcalf JEP, Jones AH, Band TJ, Skupien DS. A tribological study of cobalt chromium alloys used in metal-on-metal resurfacing hip arthroplasty. Wear 2003;255:999–1006.
8. McMinn D et al. Hip resurfacing—how metal on metal articulations have come full circle, IMechE June 2002.
9. MacDonald et al. Metal on metal versus metal on polyethylene liners in total hip arthroplasty: clinical and metal ion results of a prospective randomized clinical trial. AOA 2002;601:27–34.
10. Pfister et al. Metal ion levels from low and high carbon metal-on-metal bearings. Presented at the 7th Swiss Orthopaedic Congress, Laussane, Switzerland, 19–22 June 2002.
11. McMinn D, et al. Development of metal/metal hip resurfacing. Hip Int 2003;13;41–53.
12. Park Y-S et al. Early ostolysis following second-generation metal-on-metal hip replacement. J Bone Joint Surg Am 2005; 87:1515–1521.
13. Kovac S et al. Survivorship and retrieval analysis of sikomet metal-on-metal total hip replacements at a mean of seven years. J Bone Joint Surg Am 2006;88:1173–1182.
14. Nolan JF et al. Metal on metal hip replacement. Presented at the British Hip Society Meeting, Leeds, March 2007.

http://www.springer.com/978-1-84800-087-2

Modern Hip Resurfacing
McMinn, D.J.W. (Ed.)
2009, XVI, 432 p. 698 illus., 566 illus. in color.,
Hardcover
ISBN: 978-1-84800-087-2